Molecular Biology of the Cell
Vol. 6, 541–557, May 1995

Polarized Distribution of Actin Isoforms in Gastric Parietal Cells

Xuebiao Yao,* Christine Chaponnier,† Giulio Gabbiani,† and John G. Forte*‡

*Department of Molecular and Cell Biology, University of California, Berkeley, California 94720; and †Department of Pathology, University of Geneva, CH-1211 Geneva 4, Switzerland

Submitted November 18, 1994; Accepted March 13, 1995
Monitoring Editor: Thomas D. Pollard

The actin genes encode several structurally similar, but perhaps functionally different, protein isoforms that mediate contractile function in muscle cells and determine the morphology and motility in nonmuscle cells. To reveal the isoform profile in the gastric monomeric actin pool, we purified actin from the cytosol of gastric epithelial cells by DNase I affinity chromatography followed by two-dimensional gel electrophoresis. Actin isoforms were identified by Western blotting with a monoclonal antibody against all actin isoforms and two isoform-specific antibodies against cytoplasmic β-actin and γ-actin. Densitometry revealed a ratio for β-actin/γ-actin that equaled 0.73 ± 0.09 in the cytosol. To assess the distribution of actin isoforms in gastric glandular cells in relation to ezrin, a putative membrane-cytoskeleton linker, we carried out double immunofluorescence using actin-isoform–specific antibodies and ezrin antibody. Immunostaining confirmed that ezrin resides mainly in canaliculi and apical plasma membrane of parietal cells. Staining for the β-actin isoform was intense along the entire gland lumen and within the canaliculi of parietal cells, thus predominantly near the apical membrane of all gastric epithelial cells, although lower levels of β-actin were also identified near the basolateral membrane. The γ-actin isoform was distributed heavily near the basolateral membrane of parietal cells, with much less intense staining of parietal cell canaliculi and no staining of apical membranes. Within parietal cells, the cellular localization of β-actin, but not γ-actin, isoform superimposed onto that of ezrin. In a search for a possible selective interaction between actin isoforms and ezrin, we carried out immunoprecipitation experiments on gastric membrane extracts in which substantial amounts of actin were co-eluted with ezrin from an anti-ezrin affinity column. The ratio of β-actin/γ-actin in the immunoprecipitate ($\beta/\gamma = 2.14 \pm 0.32$) was significantly greater than that found in the cytosolic fraction. In summary, we have shown that β- and γ-actin isoforms are differentially distributed in gastric parietal cells. Furthermore, our data suggest a preferential, but not exclusive, interaction between β-actin and ezrin in gastric parietal cells. Finally, our results suggest that the β- and γ-actin–based cytoskeleton networks might function separately in response to the stimulation of acid secretion.

INTRODUCTION

Actin is one of nature's most abundant and highly conserved proteins. Actin is implicated as playing an essential role in a variety of cellular processes such as maintaining cell shape, cell motility, and cytokinesis. In mammals, there are at least six different actin isoforms, each encoded by a separate gene, and they differ by <10% of the amino acid sequence (Vandekerckhove and Weber, 1978). The isoforms include the two smooth muscle actins, α and γ, expressed primarily in

‡ Corresponding author: Department of Molecular and Cell Biology, 241 LSA, University of California, Berkeley, CA 94720.

vascular and visceral smooth muscle, respectively, whereas α-skeletal actin and α-cardiac actin are found in skeletal and cardiac muscle, respectively. In mammalian nonmuscle cells the predominant isoforms are cytoplasmic β-actin and cytoplasmic γ-actin. Although six actin isoforms exist and are regulated in their tissue-specific expression, the biological significance of these isoforms remains unknown. Major structural differences exist in their N-terminal region, and these differences are important because of the N-terminal role in binding myosin and other actin-binding proteins (Vandekerckhove, 1990). In addition, recent crystallographic studies reveal several differences in the subdomain structure of cytoplasmic β-actin and α-skeletal actin (Schutt *et al.*, 1993). Such structural comparisons might provide insights into the physiological significance of the isoforms caused by the small difference in primary sequences.

Cytoplasmic β- and γ-actin isoforms in nonmuscle cells are present in amounts that vary among different cell types (Firtel 1981; Vandekerckhove and Weber, 1981). Although there have been speculations on differential functions and/or subcellular localizations (Pardo *et al.*, 1983), differences in isoform distribution and function have been minimally explored. A differential distribution of actin isoforms has been suggested based on observed enrichment of β-actin at the cell periphery (DeNofrio *et al.*, 1989; Hoock *et al.*, 1991). The mRNA encoding β- and γ-actin isoforms were found to be differentially distributed in myoblasts (Hill and Gunning, 1993), whereas these same authors did not detect a spatial separation of the expressed protein isotypes. Two major obstacles to defining a differential distribution of actin isoforms are the development of the means to specifically probe the isoforms and the system in which cytoplasmic β- and γ-actin isoforms are spatially separated. Cytoplasmic β- and γ-actin isoform-specific antibodies have now been developed and proven to be powerful tools for localizing actin isoforms in situ (Herman and D'Amore, 1985; Otey *et al.*, 1986; Herman, 1988, 1993; DeNofrio *et al.*, 1989; Hoock *et al.*, 1991). Recently, North *et al.* (1994) used antibodies specific for cytoplasmic β-actin and muscle actin to show distinct, isoform-specific compartments in smooth muscle.

It was of interest to determine if there was a differential distribution of cytoplasmic β- and γ-actin isoforms in polarized epithelial cells where the morphology and functional properties, apical and basolateral membrane, are suited for such studies. Gastric glands are tubular structures in which the epithelial cells (parietal cells and chief cells) are organized along a central lumen. In parietal cells the distribution of filamentous actin (F-actin) is polarized toward the apical plasma membrane where actin-based microvillar structures are present. When the cells are stimulated to secrete acid, a dramatic extension of apical plasma membrane occurs after the recruitment of H,K-ATPase–containing cytoplasmic membranes (Hanzel *et al.*, 1991). Ezrin, a putative actin-binding protein, co-localizes with filamentous actin in the apical membrane of parietal cells, and has been implicated in stimulation-mediated membrane-cytoskeletal interaction (Urushidani *et al.*, 1989; Hanzel *et al.*, 1991). Activation of parietal cells was also correlated with the phosphorylation of ezrin. Although the cellular co-localization of ezrin/F-actin has now been well documented in a variety of cells, the functional relevance of ezrin in membrane volatile remodeling is still uncertain. In particular, an interaction between wild-type ezrin and F-actin has not yet been reconstituted in vitro, although a weak interaction was observed between ezrin and skeletal α-actin at low salt conditions as judged by sedimentation assay (Bretscher, 1983). More recently, using recombinant GST fusion proteins with various N-terminal deletions, Turunen *et al.* (1994) showed that the immobilized C-terminus of ezrin retains filamentous cytoplasmic actin and skeletal muscle actin on glutathione beads, and the association of actin with the truncated ezrin was relatively strong, even resistant to ionic detergents. Because ezrin is so abundant in parietal cells, especially localized to the apical and canalicular plasma membrane, and there exists the possibility of preferential interaction with actin isoforms, it was of interest to probe gastric parietal cells to ascertain the distribution and functional relevance of actin isoforms. Here we present evidence for a polarized distribution profile of cytoplasmic β- and γ-actin isoforms in gastric parietal cells. Moreover, we also show a preferential co-localization of β-actin with ezrin in the apical plasma membrane of parietal cells. Finally, we demonstrate that a substantial amount of actin co-eluted with ezrin from anti-ezrin affinity chromatography. Distinct cellular distribution of actin isoforms may provide a clue to the functional relevance of the isoforms.

MATERIALS AND METHODS

Isolation of Rabbit Gastric Glands

Rabbit gastric glands were isolated as originally described by Berglindh and Obrink (1976), and more recently by our laboratory (Urushidani *et al.*, 1989). Glands were maintained in a physiologically resting state with 10^{-5} M cimetidine.

Preparation of Gastric Cellular Fractions

Gastric cellular fractions were prepared according to Reenstra and Forte (1990). Briefly, the gastric mucosa from resting New Zealand White rabbits was minced and homogenized in hypotonic homogenizing buffer: 125 mM mannitol, 40 mM sucrose, 1 mM EDTA, 5 mM piperazine-*N*,*N*′-bis(2-ethanesulfonic acid) (PIPES)-Tris, pH 6.7. The homogenate was spun at 80 × *g* for 10 min to remove whole cells and debris. The supernatant was collected and spun at 4300 ×

g for 10 min, and the plasma membrane-rich pellet, designated as P1, was retained. The supernatant from the 4300 × g spin was then cleared of remaining organelles by centrifugation at 48,000 × g for 90 min. The supernatant from the 48,000 spin, representing the gastric cytosol, is called S3.

Antibodies

The monoclonal antibodies against ezrin, 6H11, and 4A5, were described earlier (Hanzel *et al.*, 1989). The monoclonal anti-actin antibody, C4, which recognized all mammalian actin isoforms, was described by Lessard *et al.* (1983). Another clone of monoclonal antibody against all actin isoform was obtained from Amersham (Arlington Heights, IL). Antibodies against cytoplasmic β-actin isoform were generated by immunizing rabbits with the corresponding hemocyanin-coupled NH_2 terminal nonapeptide and purified by affinity chromatography, using the nonapeptide covalently linked to Mini-Leak beads (Kem-En-Tec A/S, Copenhagen, Denmark) according to the manufacturer's description (Chaponnier, Benzonana, and Gabbiani, unpublished data). The antibody against γ-cytoplasmic actin isoform has been described earlier (Chaponnier and Gabbiani, 1989). In addition to recognizing γ-cytoplasmic actin, this antibody reacts with α- and γ-smooth muscle actin, but it does not react against β-cytoplasmic actin. Thus, in the context of the present studies only the reactivity with γ-cytoplasmic actin is relevant as smooth muscle cells are not present in the gastric glandular epithelium.

Two-dimensional Electrophoresis and Immunoblotting

Two-dimensional (2-D) electrophoresis was performed as described by O'Farrell (1975). Briefly, isolated gastric glands were solubilized in isoelectric focusing (IEF) sample buffer (9.5 M urea, 5% β-mercaptoethanol, 2% NP-40, and a mixture of 2% ampholines (vol/vol, Sigma, St. Louis, MO) consisting of two parts of pH 4–6.5 and one part of 2% of pH 3–10). The tube gels were made by using pre-mixed frozen analytical IEF solution (Millipore, Bedford, MA). Calibration of 2-D electrophoresis was done using a carbamylated calibration kit (Pharmacia, Piscataway, NJ) and using 2-D electrophoretic standard proteins, including skeletal muscle α-actin, as an internal calibration (Bio-Rad, Richmond, CA). After running for appropriate intervals, the resolved tube gels were separated according to molecular weight on 9% sodium dodecyl sulfate-polyacrylamide gel electrophoresis (SDS-PAGE). For identifying actin isoforms in gastric cytosol, the S3 supernatant proteins were applied to a DNase I–linked Sepharose column, subjected to extensive washing, and eluted with 40% formamide (Wolosin *et al.*, 1983). Eluted proteins were precipitated with 80% acetone, solubilized in IEF sample buffer, and separated by 2-D electrophoresis. The 2-D gels were stained with Coomassie blue (G-250) or post-stained with silver, while parallel sets of gels were transferred onto a polyvinylidene difluoride (PVDF) membrane (Millipore) for immunoprobing with various antibodies against actin or ezrin (Urushidani *et al.*, 1989).

Fluorescent Staining and Light Microscopy

Previous data have shown that ezrin is co-localized with F-actin within gastric parietal cells. Because the immuofluorescence using anti-actin antibodies gives the total signal from both monomeric actin (G-actin) and F-actin, we carried out two kinds of immunofluorescence: one recognizing both G- and F-actin in which the cells were fixed then carried through immunostaining; the other in which cells were extracted with a mild nonionic detergent, to remove G-actin and other soluble proteins, before fixation and immunostaining. For the latter case, we first extracted glands with NP-40 extraction buffer (0.1% NP-40, 100 mM PIPES, pH 6.9, 0.18 g/ml glycerol, 1.2 mM $MgCl_2$, 2 mM EGTA, 5 μM calpain inhibitor I, 1 mM phenylmethylsulfonyl fluoride, 1 mM pepstatin A), then fixed the glands with 4% formaldehyde, and finally settled the glands onto polylysine-coated coverslips as described by Hanzel *et al.* (1991). The extraction caused no change in the distribution of F-actin (phalloidin) or ezrin, but did tend to improve clarity of stain. Nonspecific binding was minimized by incubation with phosphate-buffered saline (PBS) containing 0.5% Tween for 15 min. Incubations with primary antibodies were for 60 min followed by three washes with PBS containing 0.5% Tween. Ezrin was visualized by secondary antibody conjugated to fluorescein isothiocyanate (FITC) or rhodamine (Jackson ImmunoResearch, West Grove, PA). β-Actin and γ-actin were separately visualized by Texas red- or FITC-streptavidin (Vector, Burlingame, CA) after incubation with biotinylated secondary antibody (Vector). In some cases, rhodamine-phalloidin (Molecular Probes, Eugene, OR) was used to localize F-actin in the glands. After processing, coverslips were mounted on slides in 1.5% Hanker/Yates antiquench medium (Polysciences, Warrington, PA) and sealed with nail polish.

Cells were examined with a Nikon epifluorescence microscope with 40X and 60X objectives, and photographs were recorded on Ektachrome and technical pan film (Eastman Kodak, Rochester, NY). Digital images of fluorescent markers were also obtained on a Zeiss microscope equipped with a computer-controlled mechanism to focus a Nikon 60X objective lens and a cooled CCD camera (Scanalytics, Billerica, MA) as described by Fay *et al.* (1989). Glands were double labeled by indirect immunofluorescence using antibodies against ezrin and either β-actin or γ-actin, as described above. Images were collected as a series of optical sections with a spacing of 0.5 μm in the z-axis through the 35- to 40-μm thickness of the gland. Thus, 70–80 sections were collected for one fluorophore and the optical sectioning was repeated for another 70–80 sections for the other fluorophore. All raw images were stored on a computer and could be viewed individually, or as an entire stacked data set for a three-dimensional view. To minimize out-of-focus light the raw images were restored using a deconvolution algorithm described by Carrington *et al.* (1990) to estimate the true distribution of fluorescence in each plane. Calibration of blurring produced by the microscope optics was determined by measuring the point spread function of 0.19-μm diameter latex beads labeled with the same fluorophores as for the experimental data and collected through a series of optical sections taken at 0.5-μm intervals.

Affinity Chromatography

Ezrin was immunoprecipitated by either of two general methods: using monoclonal antibody 6H11 covalently linked to Affi-Gel 10 beads or using immobilized protein G. 6H11 was linked to Affi-Gel 10 beads (Bio-Rad) as described by the manufacturer. Briefly, the precipitate of ascites containing 6H11 was dialyzed against distilled water and 0.1 M *N*-2-hydroxyethylpiperazine-*N'*-2-ethanesulfonic acid, pH 8.0. The beads were gently mixed with 6H11 for 4 h at 4°C. The 6H11-coupled beads were washed with PBS then incubated with 1 M ethanolamine, pH 8.0, for 1 h to block excess unreacted *N*-hydroxysuccinimide groups. The affinity column was stored at 4°C in PBS containing 0.1% NaN_3. Before each run, the column was washed with elution buffer and re-equilibrated with PBS before applying gastric membrane extracts. When immunoprecipitation was conducted using protein G, the Protein G-Sepharose beads (Boehringer Mannheim, Indianapolis, IN) were incubated with anti-ezrin 6H11 for 1 h on ice. After extensive washing with PBS, the two types of beads were incubated with ezrin-containing membrane fractions. To test if actin was trapped nonspecifically by antibody-affinity beads, we performed a control experiment in which a monoclonal antibody G1/136 was coupled to Affi-10 beads, exactly like mAB 6H11, but for which we did not detect any cross-reacting parietal cell proteins. The procedures for conducting G1/136 and 6H11 reactions and washings were identical to those described above.

The gastric membrane fraction designated as P1, containing large organelles including apical plasma membrane fragments enriched

in ezrin, was extracted with extraction buffer containing 0.5% Triton X-100, 300 mM NaCl, 1 mM EGTA, 0.25 mM phenylmethylsulfonyl fluoride, 10 μM E64, 1 mM benzamide, 20 mM Tris-Cl, pH 7.4, on ice for 30 min and centrifuged at 20,000 × *g* for 20 min. Higher ionic strength was applied here to maximize the release of ezrin (Hanzel *et al.*, 1991). This extraction procedure released about 60–70% of the P1-ezrin to the supernatant, thus a substantial amount of ezrin remained in the detergent-insoluble pellet. Aliquots of the supernatant were mixed by gentle rotation for 2 h at 4°C with Affi-10 gel coupled with anti-ezrin antibody. The beads were washed with 3-(*N*-morpholino)propanesulfonic acid (MOPS)-buffered saline (MBS) containing 20 mM MOPS, pH 7.4, 0.1 M NaCl until OD_{280} was less than 0.01. Additional washes were carried out with MBS containing 0.5 M and 1 M NaCl, respectively, to remove nonspecific trapping. The ezrin was then eluted with 10% ethylene glycol containing 20 mM HCl, pH 3.0, or 0.1 M glycine, pH 2.8. The elutants were neutralized immediately with Tris base and concentrated by centrifugation with a Microconcentrator-30 (Amicon, Danvers, MA). For SDS-PAGE and 2-D electrophoresis, the elutants were precipitated with 80% acetone, and the precipitates were solubilized in SDS-PAGE buffer or IEF gel sample buffer.

Densitometric Analysis

For quantitation, the signals from the gels stained with Coomassie blue or with silver intensification, and blots probed with anti-actin monoclonal antibodies, were scanned with a densitometer and the data were analyzed using National Institutes of Health Image 1.47 software.

RESULTS

Characterization of Gastric Actin Isoforms

The cytoplasmic β and γ-actin isoforms co-exist in most nonmuscle cells. It has been been speculated that they differ in their in vivo function and/or subcellular localization. These two isoforms have the same molecular mass, but differ slightly in amino acid composition and isoelectric point (Herman, 1993). To test for actin isoforms in the cytosolic fraction of gastric epithelial cells, we purified monomeric actin from the S3 supernatant fraction harvested from gastric mucosal homogenates. Gastric actin was purified by DNase I-affinity chromatography and subsequent elution in 40% formamide as described by Wolosin *et al.* (1983), and then subjected to 2-D electrophoresis and sequential Western blotting. A silver-stained 2-D gel of monomeric actin from the DNase I column is shown in Figure 1, where at least four spots are seen that co-migrate at 43 kDa with different pI values ranging from about 5.23–5.10. To verify the identity of "actin" spots, we probed transblots with a monoclonal antibody C4 reactive with all actin isoforms (Lessard *et al.*, 1983). As shown in the inset to Figure 1, immunoblotting with antibody C4 gave four spots corresponding to those of the protein-stained gel, labeled γ, β, γ′, and β′ from right to left. Among a dozen similar 2-D gels and blots analyzed, we found a consistent differential intensity among the four spots; the most basic spot (estimated pI of ~5.23) bore the brightest signal, whereas the most acidic spot (estimated pI of ~5.1) was less intense. Occasionally, we also found an additional pair of less intense spots, focused with even more acidic pI values of about 5.03 and 5.0, respectively.

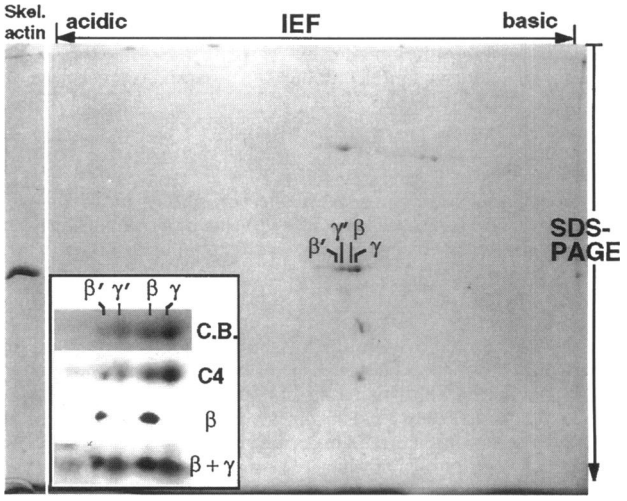

Figure 1. Identification of actin isoforms in the gastric cytosol. The supernatant fraction from gastric mucosal homogenate was subjected to DNase I chromatographic fractionation as described in MATERIALS AND METHODS. Purified gastric actin was separated by 2-D electrophoresis (IEF in one dimension and SDS-PAGE in the second dimension). A single lane of purified skeletal muscle actin was run by SDS-PAGE (left) for comparison. Proteins were either stained by Coomassie blue or transferred onto PVDF membrane for Western blotting. The main gel shows the total purified gastric actin fraction, including several spots running at equivalent M_r to skeletal muscle actin and in the pI range of 5.0–5.2. The inset is an expanded view of the actin spots seen by Coomassie blue (C.B.), and by Western blots probed with C4 antibody against all actin isoforms (C4), anti-β-actin antibody (β), and anti-γ-actin antibody after anti-β-actin antibody (β + γ). Locations of the β-actin isoforms are indicated by β and β′ and the γ-actin isoform are indicated by γ and γ′.

To determine whether gastric cytosolic actin is composed of β- and γ-actin isoforms, two parallel sets of blots were probed with isoform-specific antibodies. In the blot probed for the β-actin isoform (Figure 1, inset, labeled β), two spots were identified that co-migrated at 43 kDa with a separation distance equivalent to 0.1 pH unit. The more basic spot was brighter than the acidic spot. Probing with γ-actin antibody gave a similar profile, i.e., two spots with slightly different densities, but each spot was slightly more basic than those detected by the β-actin antibody. For simplicity, the inset in Figure 1 labeled β + γ is a doubly probed immunoblot on which the γ-actin isoform was detected after identification of the β-actin isoform. In this manner two additional distinct spots appeared, both of which were slightly basic to the respective β-actin spots. Therefore, the double probing identified four spots that corresponded to the additive signals for both β- and γ-actin isoforms. Furthermore, the doubly probed immunoblots confirmed that the γ-actin iso-

forms had more basic pI values than the β-actin isoforms, consistent with reports by several groups (Otey *et al.*, 1986; Hoock *et al.*, 1991). Our specific pI values are less than 0.1 pH unit more acidic than the corresponding values reported by Leavitt *et al.* (1980), but this small difference might be due to the use of different standards.

The β- and γ-actin antibodies each distinctly identified a pair of spots with a separation distance equivalent to ~0.1 pH unit. The unequivocal identification of separate actin spots on 2-D Western blots reinforced the specificity, without cross-reaction, of the two actin isoform antibodies used here. In addition, because identification of total actin by the C4 antibody revealed four spots that were coincident to the additive spots from β- plus γ-actin isoforms, we concluded that the gastric monomeric actin pool contains only β- and γ-actin isoforms. The identity of the "double" spot for each of the two isoforms is presently uncertain. The more acidic spots might represent phosphorylated forms of the respective actin isoforms, or there may be some other unaccounted for artifactual change in preparing the material.

The data in Figure 1 also suggest that gastric cytosol might contain higher levels of γ-actin isoform than β-actin isoform. To estimate the ratio of β-actin isoform to γ-actin isoform in the gastric cytosol, we carried out densitometric analysis on 2-D gels of the DNase I–purified material from the cytosolic S3 fraction of five gastric mucosal preparations. The measured ratio of β-actin/γ-actin was 0.73 ± 0.09 ($p < 0.05$). Because the cytosol contains primarily soluble actin, this suggests that there is slightly more γ-actin isoform than β-actin isoform in the monomeric pool.

Differential Distribution of Actin Isoforms in Gastric Glandular Cells

Our previous studies have characterized the distribution of filamentous actin in gastric glandular cells (Wolosin *et al.*, 1983; Hanzel *et al.*, 1991). Because actin isoforms were clearly represented in the gastric extracts, it was of interest to determine if an isoform-specific distribution of β- and γ-actin could be detected within the cells using immunofluorescence microscopy. To optimally visualize the cytoskeletal actin isoforms, gastric glands were extracted with NP-40 solution before fixation and subsequent immunofluorescent probing: a preparation we refer to as permeabilized glands. The images of differential-interference-contrast (PIC) in Figure 2, a and c, provide a perspective of the glandular organization in which the focus is through the middle of the gland. The corresponding glands probed with either β- or γ-actin-specific antibodies are shown in Figure 2, b and d, respectively. The lumen of a gastric gland is a centralized tubule-like structure formed by the apices of the surrounding epithelial cells, including parietal cells, chief cells, and mucous neck cells. Parietal cells are easily visualized as larger cells, often protruding from the gland. Chief cells and mucous neck cells cannot be distinguished from one another in this microscopic format, but they are collectively identified as smaller, more centrally located, cells. The plasma membrane facing the lumen is designated as the apical membrane, and the membrane between the cells and facing the bath is the basolateral membrane. In permeabilized glands probed for β-actin shown in Figure 2b, parietal cells exhibit intense staining of an intracellular network reminiscent of the apical plasma membrane that is sequestered in the form of the intracellular canaliculi. In addition, a rather intense β-actin immunofluorescence was clearly identified along the entire gland lumen, indicating localization to the apical membrane of all gastric epithelial cells. The basolateral surfaces of parietal cells were also stained by β-actin antibodies, and very light staining for β-actin was seen near the basolateral membranes of nonparietal cells. The pattern of immunofluorescence in glands probed for γ-actin was distinctly different from that of β-actin. Only parietal cells showed an appreciable amount of γ-actin immunofluorescence, which was typically visualized as a ring-like structure adjacent to the basolateral membrane (Figure 2d). Often the pattern of γ-actin staining in the parietal cell was seen as a double-ringed structure: a heavily stained outer continuous ring proximal to the basolateral membrane, and a more lightly stained discontinuous inner structure extending deeper into the cell corresponding to the apical intracellular canalicular membrane. Immunostaining of nonparietal cells with the γ-actin antibodies was weak and confined to their basolateral plasma membranes. We have also probed gastric glands with the same general procedure, but using a monoclonal antibody against smooth muscle α-actin; however, no visible staining occurred, which corresponded to the negative result from 2-D Western blotting. In sum, there is a differential distribution of β- and γ-actin isoforms in gastric glandular cells: β-actin is concentrated in the apices of all gastric epithelial cells, including the canalicular membrane of parietal cells, while γ-actin is more prominent at the basolateral surface, with minor deposition in the region of the secretory canaliculi of parietal cells.

Distribution of Actin Isoforms in Relation to Total F-Actin in Gastric Parietal Cells

Previous studies in gastric glands demonstrated that F-actin was highly represented in parietal cells, with primary localization to the apical canalicular membrane of parietal cells as well as the apices of nonparietal cells, and less intense staining at the basolateral surfaces (Hanzel *et al.*, 1991). In fact, this pattern of

F-actin staining was similar to that noted above for glandular β-actin localization. To directly compare the localization of total F-actin with that of the actin isoforms we carried out double labeling on permeabilized glands by which F-actin was visualized by FITC-conjugated phalloidin and the actin isoforms were separately visualized by Texas-red–linked streptavidin. As seen in Figure 3a, β-actin is localized at the apical and canalicular membrane of parietal cells as well as the apices of nonparietal cells. Basolateral staining of β-actin in nonparietal cells is barely visible, whereas a basolateral distribution of β-actin in parietal cells is clearly identified. The distribution of F-actin in the same glands is virtually superimposed onto that of β-actin (Figure 3b); a minor distinction between these two signals is usually seen as a slightly higher contrast and brighter lumenal staining for F-actin compared with that of β-actin. Figure 3c shows the typical staining for γ-actin and F-actin in permeabilized glands. Staining for γ-actin is prominently localized at the basolateral surface of parietal cells with minor deposition at the secretory canalicular membrane and no staining of the gland lumen. There was very little concordance in the distribution of F-actin with γ-actin near the luminal aspects of the cells. However, there was some co-localization of F-actin with γ-actin toward the basolateral surfaces of parietal cells.

Figure 4 shows the comparable double staining for β-actin and F-actin (Figure 4, a and b) and for γ-actin and F-actin (Figure 4, c and d) in glands that were not permeabilized with NP-40 before fixation. The respective patterns for β- and γ-isoform distribution were similar to their permeabilized counterparts as shown in Figure 3, except that the images were often somewhat less sharp presumably due to higher content of cytosolic protein.

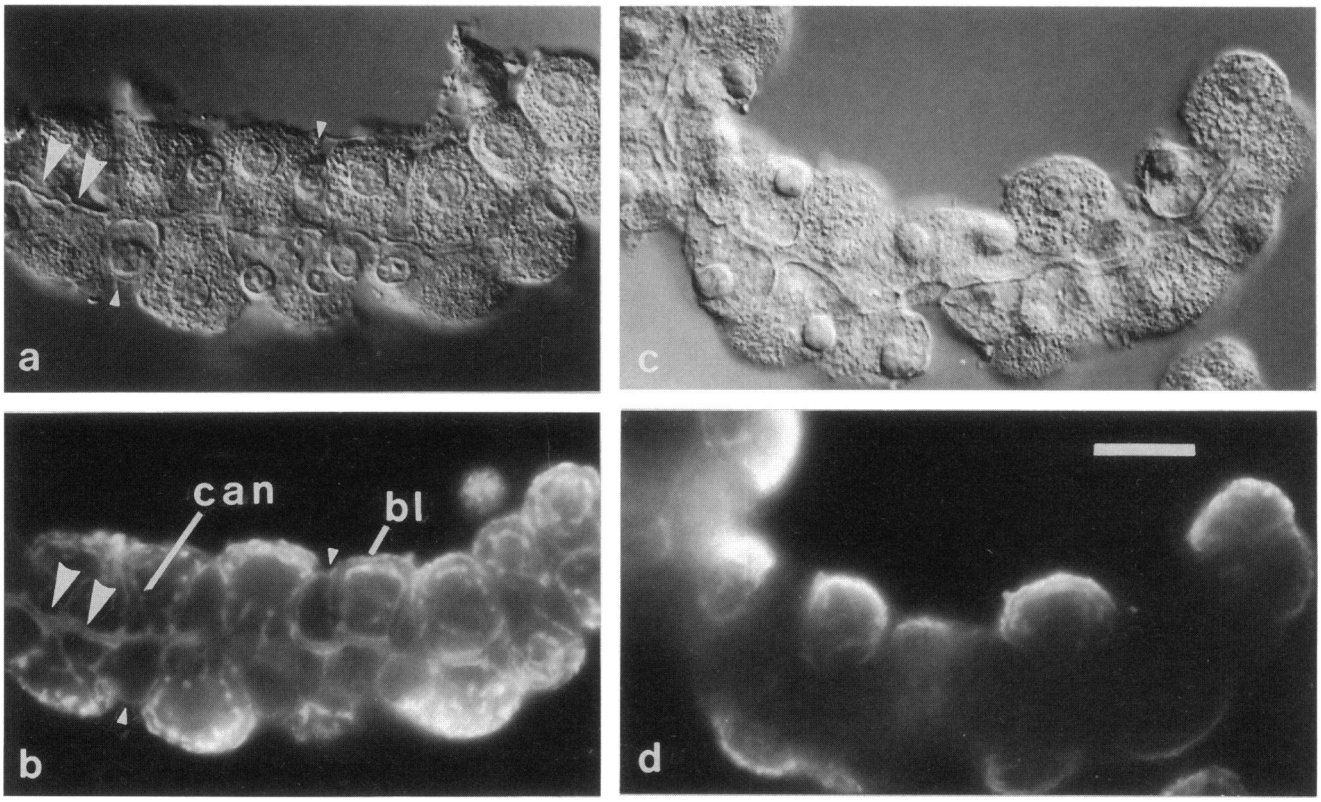

Figure 2. DIC microscopy and immunofluorescence of isolated gastric glands probed for β- and γ-actin isoforms. NP-40 extracted glands were probed with antibodies for either β-actin (a and b) or γ-actin (c and d), followed by secondary antibody conjugated to FITC. The DIC images (a and c) and the fluorescent images (b and d) were focussed at the same plane near the central lumen of the gland. The tubule-like gland lumen is seen throughout the gland (large arrowheads). Parietal cells are easily recognized as the larger cells protruding from the lumen, whereas the chief cells and/or neck cells are seen as smaller centrally located cells (small arrowheads). For the β-actin immunofluorescent labeling (b) parietal cells are heavily stained throughout the network of intracellular canaliculi (can) and an outer ring near the basolateral plasma membrane (bl). In addition, β-actin staining occurs along the entire glandular lumen (large arrowheads), localized to the apices of the smaller epithelial cells (small arrowheads) that line the lumen; basolateral plasma membranes of the smaller cells are very lightly stained. Immunofluorescent labeling of γ-actin (d) is heavily localized to the basal and lateral regions of parietal cells. A light staining can sometimes be seen approximating the canalicular membrane. No staining for γ-actin is seen along the gland lumen. Bar, 20 μm.

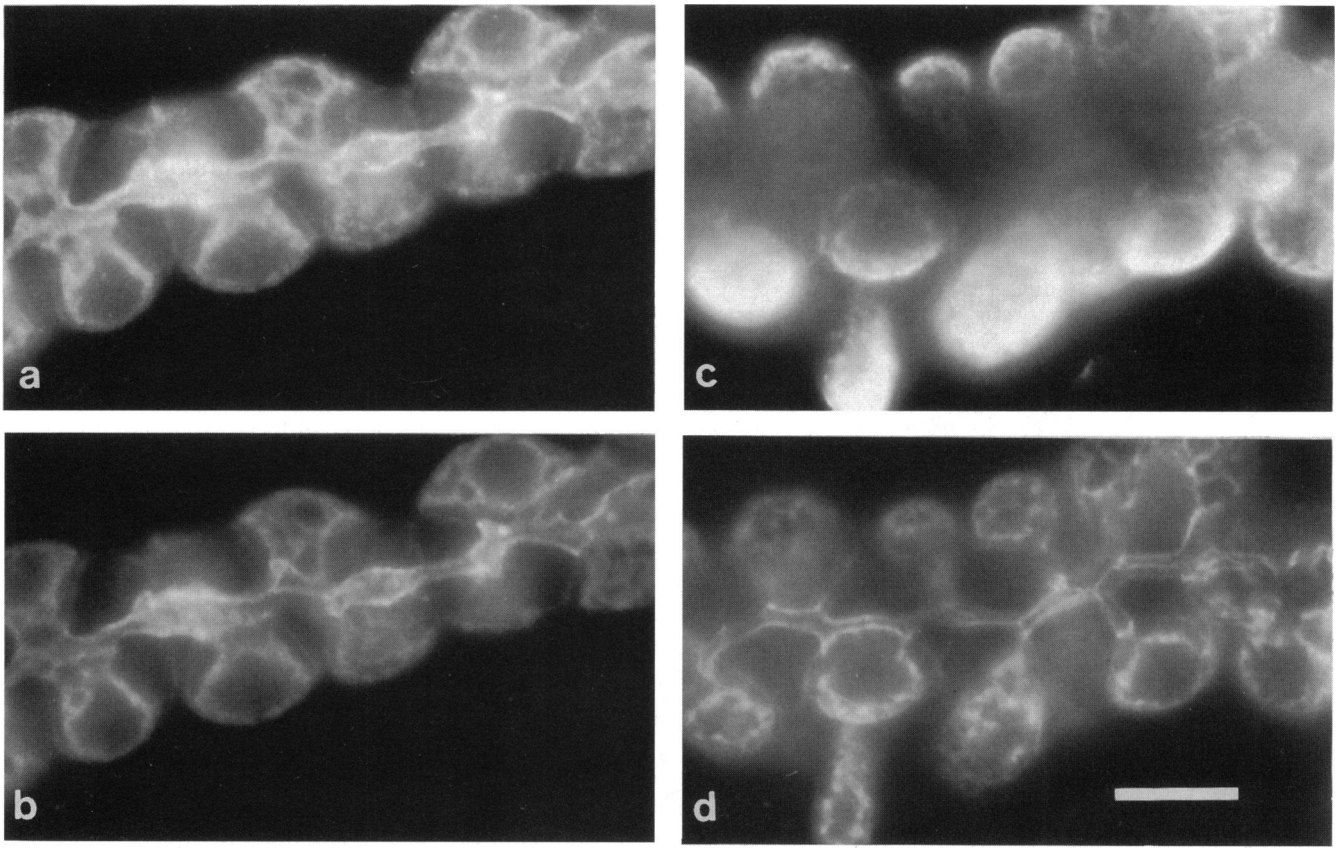

Figure 3. Localization of actin isoforms in relation to total F-actin in gastric glandular cells extracted with NP-40 before fixation. Gastric glands were first extracted with NP-40 as described in MATERIALS AND METHODS to eliminate most cytosolic protein, then fixed and either double probed for β-actin (a) and F-actin (b), or γ-actin (c) and F-actin (d). The glands were incubated with either anti-β-actin or anti-γ-actin antibody followed by biotinylated goat anti-rabbit antibody and Texas red-streptavidin. Visualization of total F-actin was then accomplished by respective FITC-phalloidin labeling. Immunofluorescence of β-actin (a) very closely parallels the pattern of F-actin staining (b): prominent along the gland lumen and within the apical and canalicular membranes of parietal cells. Immunofluorescence of γ-actin (c) is most prominent at the basolateral membrane of parietal cells with lighter staining of the intracellular canaliculi and virtually no staining of the gland lumen. The γ-actin pattern contrasts with the double probed image of F-actin staining (d). Bar, 20 μm.

Co-localization of Ezrin with β- and γ-Actin Isoforms in Gastric Glandular Cells

Previous studies in gastric glands demonstrated that ezrin was almost exclusively confined to parietal cells, and that its distribution was primarily to the apical canalicular membrane with less intense staining to the basolateral surface (Hanzel *et al.*, 1991). Because the β-actin isoform also appeared to predominate in the canalicular membrane of parietal cells, we undertook a co-localization study of β-actin and ezrin. We carried out two sets of double immunofluorescence of permeabilized glands in which ezrin was localized with a mouse monoclonal antibody (6H11) and either β-actin or γ-actin were localized with the isoform-specific antibodies described above. As reported earlier by Hanzel *et al.* (1991), and shown in Figure 5, b and d, ezrin was concentrated in the branching network that is characteristic of the apical and secretory canalicular membrane of parietal cells, and in lesser quantities at the basal surface of parietal cells. Also, ezrin was not found in any gastric epithelial cell other than parietal cells. Simultaneous probing with the β-actin antibody showed a pattern of staining within the parietal cell that was nearly identical to that of ezrin (Figure 5a). However, unlike ezrin, β-actin staining was also present at the apices of all epithelial cells lining the lumen of the glands and β-actin staining was also observed to a much lower degree at the basolateral membrane of the nonparietal cells. Thus, the distribution of β-actin is superimposed onto that of ezrin within parietal cells, as well as being found in other gastric epithelial cell types.

Double immunofluorescence probing for ezrin and γ-actin is exemplified in Figure 5, c and d. As

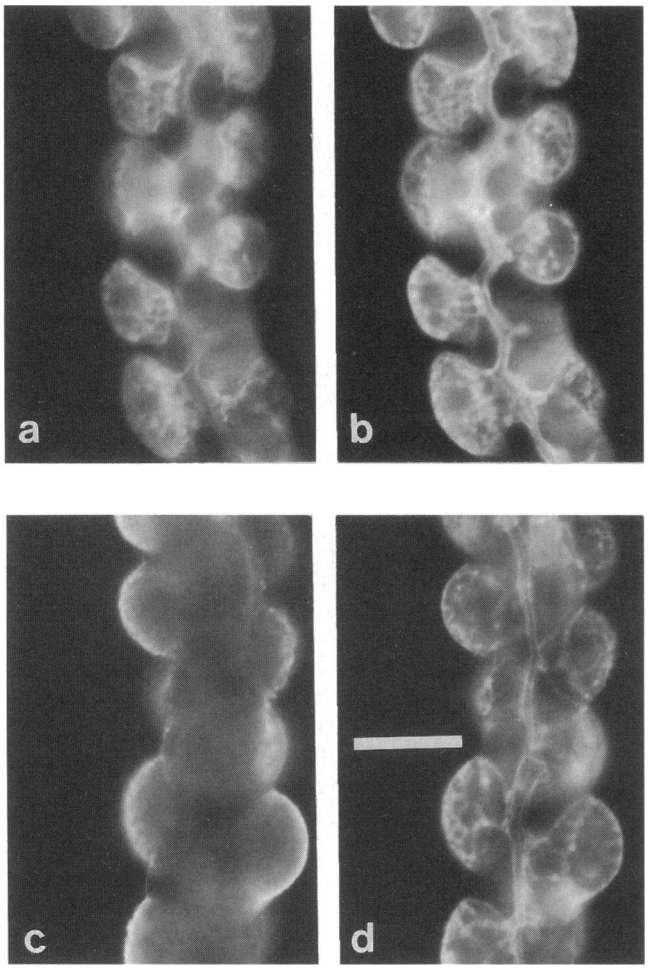

Figure 4. Localization of actin isoforms and total F-actin in gastric glandular cells that were fixed before permeabilization. Fresh gastric glands were immediately carried through the formaldehyde fixation before being permeabilized and probed as described in Figure 3. The presence of cytosolic proteins in these unextracted cells makes the fluorescent images somewhat less sharp than for detergent-extracted glands, but the localization of the actin isoforms, double probed for F-actin, has not been altered: β-actin (a) more closely parallels the pattern of F-actin staining (b), primarily along the gland lumen and within the apical and canalicular membranes of parietal cells; whereas γ-actin (c) is more prominent at the basolateral membrane of parietal cells and has little correspondence to F-actin (d) stain. Bar, 20 μm.

described above, γ-actin was predominately localized to basolateral membrane sites of parietal cells, with diminished labeling extending to the networks within parietal cells. This is exactly opposite to the pattern of ezrin staining, which is more prominent at the apical canalicular networks and diminished at the basolateral surfaces. Thus, there is some minimal colocalization of ezrin and γ-actin, but in the main these proteins appear to be conversely distributed within parietal cells.

Three-dimensional Analysis of the Spatial Distribution of Actin Isoforms and Ezrin

Gastric glands are tubular structures that are several cells thick, thus epifluorescence often appears obscured by out-of-focus image. To minimize this interference, optical sections were acquired at a series of focal planes and the images were restored (deconvolved) as described in MATERIALS AND METHODS. To verify the spatial relationships among β-actin, γ-actin, and ezrin distribution, we took serial digitized images from double-stained glandular cells over the full thickness of the gland (35–40 μm) with a z-axis spacing of 0.5 μm. In general the data are consistent with what was observed with conventional fluorescence microscopy, with a somewhat finer degree of localization. Figure 6 shows a series of optical sections taken from identical planes for glands simultaneously probed with fluorescein-labeled anti-ezrin antibody and rhodamine-labeled anti-β–actin antibody. For simplicity the figure includes only every 8th section from the series taken from the gland bottom to the surface. In the central region of the gland (Figure 6, d–f and d′–f′) β-actin staining is clearly visible along the apices of all epithelial cells, thus outlining the glandular lumen. Ezrin is absent from the gland lumen, as it is absent from the nonparietal cells. Within parietal cells, β-actin and ezrin are abundant and primarily colocalized to the same regions, characteristic of the tortuous apical canalicular surface wending through most of the cell, with relatively light deposition of stain at the basolateral surface. Colocalization of parietal cell β-actin and ezrin is also apparent as the focal plane moves up or down through the gland. The optical sections shown in Figure 7 reinforce the drastic differences between the pattern of γ-actin staining and ezrin staining. Neither Ag is localized to the gland lumen, but differences within the parietal cells are strikingly obvious. As noted above ezrin is localized to the tortuous network suggestive of canaliculi. Staining for γ-actin is heavily localized to the basolateral surface with some suggestive colocalization with ezrin in the regions immediately adjacent to that surface.

Co-Immunoprecipitation of Actin Isoforms Together with Ezrin from Gastric Glands

Because ezrin spatially co-localizes with filamentous actin within the parietal cell (Hanzel *et al.*, 1991), and the present data show that it is primarily the β-actin isoform in its filamentous form that is co-localized with parietal cell ezrin, we wondered if ezrin might preferentially associate with the β-actin isoform. The low speed crude membrane fraction (P1) containing plasma membranes and enriched in ezrin was extracted with Triton X-100 and the soluble extract was subjected to immunoaffinity chromatography using an antibody against ezrin. The upper panel of Figure 8

presents Coomassie blue-stained SDS-PAGE of fractions from an immunoadsorption experiment. The figure shows that incubation of the TX-100 extract of P1 membranes with 6H11-bound beads did not result in a gross adsorption of polypeptides; most of the proteins in the starting material (sm) were represented in the nonbinding fraction (nb). When the beads were subjected to stepwise washes of 0.15 M, 0.5 M, and 1 M NaCl only scant amounts of an 80-kDa protein were eluted. Interestingly, three major polypeptide bands (80 kDa, 55 kDa, and 43 kDa) were eluted by the subsequent HCl washes. Western blots of these same fractions were probed for ezrin and actin (Figure 8, middle and lower panels). The 6H11 antibody (Figure 8, middle panel) was used to verify the 80-kDa band as authentic ezrin and that the band(s) at ~55 kDa represents a proteolytic product of ezrin as reported by Yao *et al.* (1993). The lower panel of Figure 8 shows that the 43-kDa band in the HCl-eluted fractions clearly cross-reacted with the C4 antibody, confirming this peptide as actin. In more than 10 equivalent immunoaffinity experiments using either covalently bound 6H11 anti-ezrin antibody or 6H11 bound to immobilized protein G, we obtained similar results, in which actin was released along with ezrin when the immunobeads were subjected to the HCl/ethylene glycol washes, indicating that gastric actin associates with ezrin during the course of immunoprecipitation. Interestingly, actin was not eluted from the ezrin affinity beads by extensive washing with high salt, thus suggesting a strong interaction between ezrin and gastric actin. We propose that the actin that co-precipitates with ezrin is in the filamentous form because the DNase I affinity-purified monomeric actin fraction does not contain ezrin. To test whether this filamentous actin is nonspecifically trapped by affinity beads, we performed a control experiment in which the identical NP-40 extracts of P1 membranes were incubated with Sepharose beads covalently coupled to a mouse monoclonal antibody, G1/136 (Eilers *et al.*, 1989),

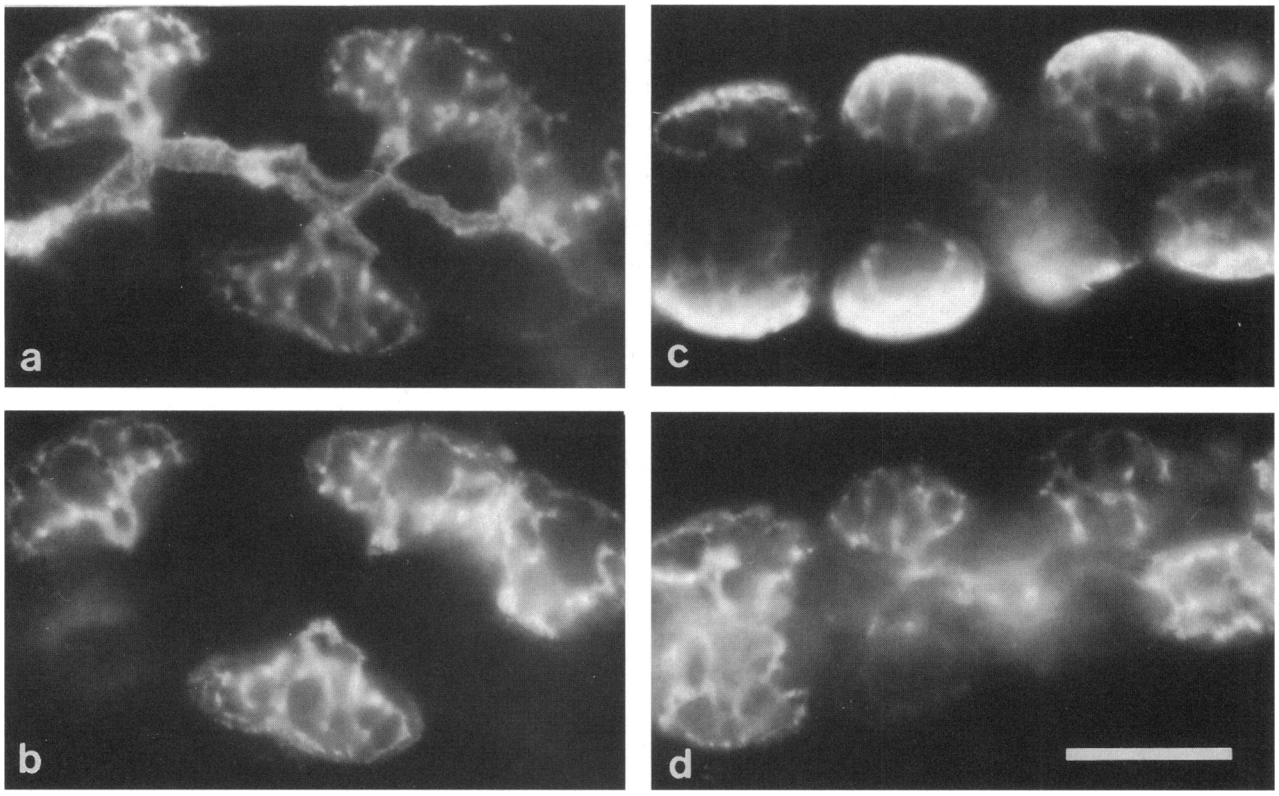

Figure 5. Ezrin is co-localized with the β-actin isoform, but not the γ-actin isoform, in gastric parietal cells. Double immunofluorescence of permeabilized glands was carried out in which either β-actin (a) or γ-actin (c) were localized with respective isoform-specific antibodies, and ezrin was localized with antibody 6H11 (b and d). Ezrin distribution was visualized by FITC-conjugated secondary antibody whereas β-actin or γ-actin localization were seen by Texas red-streptavidin. Ezrin (b and d) is confined to parietal cells, concentrated in the branching network that is characteristic of the apical and secretory canalicular membranes, and in lesser quantities at the basolateral surfaces. Simultaneous probing with the β-actin antibody (a) showed a pattern of staining that was nearly identical to that of ezrin within the parietal cell. Unlike ezrin, β-actin was also localized along the entire gland lumen formed by the apices of nonparietal cells. Immunofluorescence of γ-actin (c) was predominantly localized to the basolateral region of parietal cells, with diminished labeling extending to the networks within parietal cells. This contrasts with ezrin, which is prominent at the intracellular canaliculi and diminished at the basolateral surfaces. Bar, 20 μm.

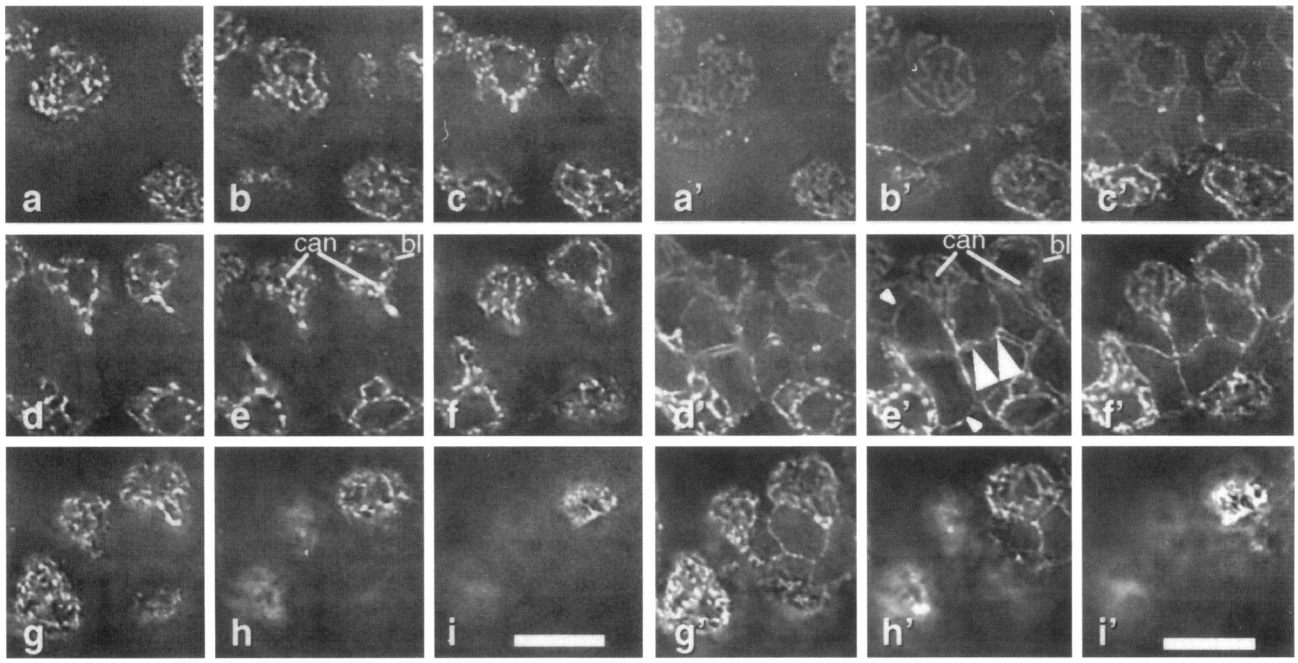

Figure 6. Ezrin is co-localized with the β-actin isoform adjacent to the apical and canalicular membranes of parietal cells. The double montage represents a series of optical sections, spaced about 3–4 μm in the z-axis, from the bottom (a and a′) to the top (i and i′) of a gastric gland doubly stained for ezrin (a–i) and cytoplasmic β-actin isoform (a′–i′). Ezrin is located only within parietal cells; within parietal cells there is a high coincidence in the localization of ezrin and β-actin, in a pattern suggestive of the tortuous infoldings of the apical plasma membrane forming the intracellular canaliculus (can). Somewhat lighter staining of ezrin and β-actin can be seen near the basolateral membrane (bl) of parietal cells. Distinct from ezrin, β-actin can be identified along the entire gland lumen (large arrowheads), consistent with a distribution to the apical microvilli of chief cells or mucous neck cells intervening between parietal cells. There is also some light β-actin staining near the basolateral membranes of the nonparietal cells (small arrowheads). Individual fluorescent images from each focal plane were digitally collected and stored on a computer. The images were subsequently corrected for out-of-focus blurring using a point spread function generated for each fluorphore and a deconvolution routine described by Carrington *et al.* (1990). Bar, 15 μm.

against a membrane protein that we found not to be present in parietal cells. When the same protocol was applied to the G1/136 affinity column as shown in Figure 9, neither ezrin nor actin remained associated with the column, indicating that actin is not passively trapped by the nonspecific IgG or the beads. Thus, we conclude that gastric actin is associated in complex with ezrin.

To further probe the actin-ezrin co-immunoprecipitation and to test whether any actin isoform preferentially co-elutes with ezrin, we separated the immunoprecipitates by 2-D electrophoresis. The gels were transferred onto the PVDF membrane and the blots were probed for ezrin with the 6H11 antibody and either the γ-actin isoform, the β-actin isoform, or both. In Figure 10 the major blot probed for ezrin shows a cluster of six closely migrating spots, with an M_r-80 kDa, separated from one another by an estimated 0.1 pH unit ranging from 6.2 to 6.7. These 80-kDa spots clearly represent ezrin in the typical 2-D separation profile that is characteristic of phosphorylated isotypes of ezrin (Hanzel *et al.*, 1991). Moreover, the 6H11-antibody–positive spots, migrating at 55 kDa in the range of pH 6.9 to 6.7, represent proteolytic products of ezrin as reported by Yao *et al.* (1993). The portion of the blot probed for γ-actin shows a major spot with an M_r-43 kDa in the pH range of ~5.2, and a minor slightly more acidic spot. In parallel blots probed for β-actin (Figure 10, white border inset) the major and minor spots at 43 kDa were shifted slightly more acidic than the γ-actin probing. Thus both β- and γ-actin isoforms are co-purified with ezrin by means of immuno-affinity chromatography. To estimate the relative amounts of actin isoforms, silver-stained 2-D gels were scanned by densitometry. In four experiments on silver-stained 2-D gels similar to that exemplified in the inset to Figure 10 (black border), we derived a mean ratio for β-actin to γ-actin of 2.14 ± 0.32 ($p < 0.01$). Because this ratio of β/γ-actin from the immunoprecipitation was almost three times higher than the β/γ ratio in the DNase I-purified monomeric actin pool, we carried out densitometric analyses on 2-D Western blots probed for all actin isoforms from several other cell fractions. Table 1 summarizes the mean ratios for β-actin to γ-actin for total gastric gland extract, the gastric cytosolic S3 fraction (rich in G-actin), the plasma membrane-rich P1 fraction (rich in F-actin), the TX-100 extract from the P1 fraction (that

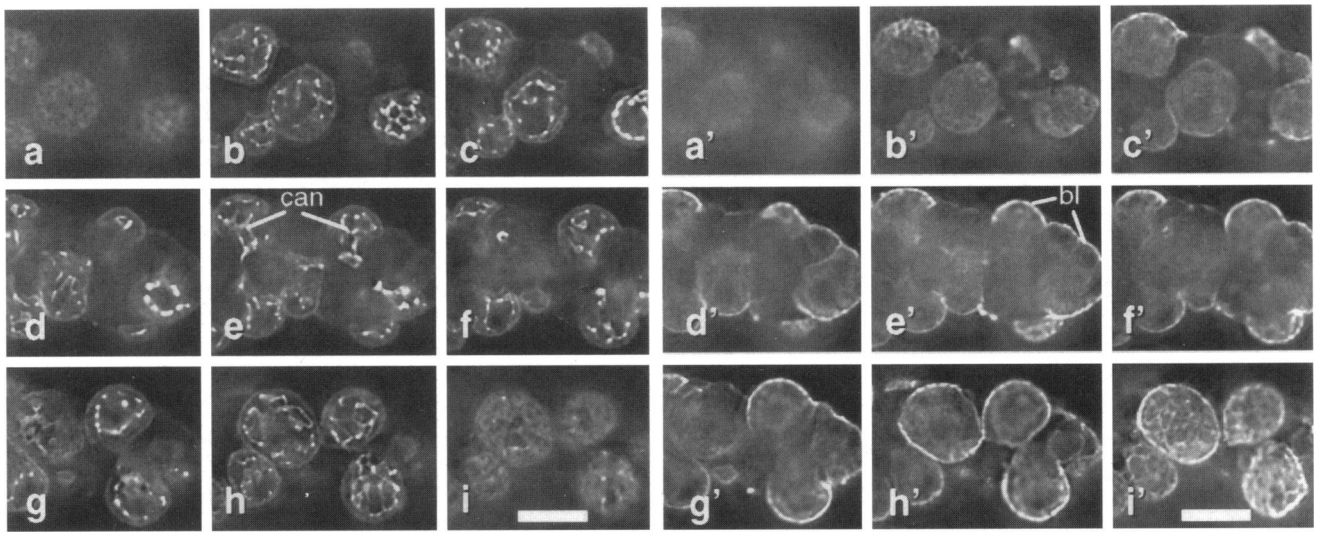

Figure 7. Distribution of parietal cell ezrin is distinctly different from the distribution of γ-actin. This double montage of optical sections is arranged similarly to that shown in Figure 5, but in this case the gastric glands were doubly stained for ezrin (a–i) and the cytoplasmic γ-actin isoform (a'–i'). Ezrin is principally localized to the intracellular canaliculi (can) of parietal cells, with a distribution markedly distinct from γ-actin. γ-Actin is most highly represented near the basolateral membrane (bl) of parietal cells, with lighter staining of interior parietal cell structures and basal membranes of nonparietal cells. Images were collected as described in Figure 5 and MATERIALS AND METHODS. Bar, 15 μm.

which was reacted with 6H11 mAb), and the final eluted material from the immunoprecipitation. In total gastric glands there is only a slight excess of β-actin over γ-actin. However, as seen from Table 1, β-actin preferentially partitions into the plasma membrane fraction (P1) whereas γ-actin is preferentially distributed to the cytosolic fraction (S3). In addition, the ratio of β/γ-actin did not change significantly ($p > 0.05$) during the course of NP-40 extraction and immunoprecipitation. Furthermore, the ratio of β/γ-actin derived from immunoprecipitation reinforces the observation of immunofluorescence in which ezrin was superimposed onto β-actin. These data are consistent with a tight interaction between ezrin and filamentous actin, with a possible preference for β-actin over γ-actin, although the nature of interaction awaits further study.

DISCUSSION

The cytoplasmic β-actin and γ-actin isoforms co-exist in most nonmuscle cells. It has been speculated that the isoforms differ in their in vivo function and/or subcellular localization (Pardo *et al.*, 1983; Toyama and Toyama, 1984). Here we show that the cytoplasmic β- and γ-actin isoforms co-exist in gastric parietal cells and comprise the total actin present in the gastric epithelium. Furthermore, we provide the first demonstration that cytoplasmic β- and γ-actin isoforms are differentially polarized in all gastric epithelial cells. In addition, our data show that in parietal cells the distribution profile of β-actin isoform closely superimposes onto that of ezrin. Finally, we demonstrate that the ezrin is associated biochemically with gastric actin, with possible preferential interaction with the β-actin isoform.

A major role for actin-based cytoskeleton in the secretory processes of parietal cells has been implied from studies showing that cytochalasin B disorganized actin filaments within the apical canalicular membrane and inhibited HCl secretion (Black *et al.*, 1982). Highly organized microfilaments are a characteristic feature of microvilli within the parietal cell canaliculus; however, the concentric arrangement of the actin filaments in proximity to the plasma membrane of parietal cell microvilli is distinctly different from the central-core localization of actin filaments in intestinal microvilli, and may be related to the greater functional plasticity of parietal cell microvilli (Black *et al.*, 1982; Forte and Soll, 1989). In going from a resting state to secretory activity, there are major changes in the apical surface area of parietal cells, including long extended microvilli, but few ultrastructural changes have been noted in the microfilament organization with the exception of possible cross-bridges between microfilaments and microvillar membrane. Interestingly, as parietal cells return to the resting stage, after removal of stimulants, microfilament ultrastructural changes become more apparent as a disorganization of the actin filaments and collapse of

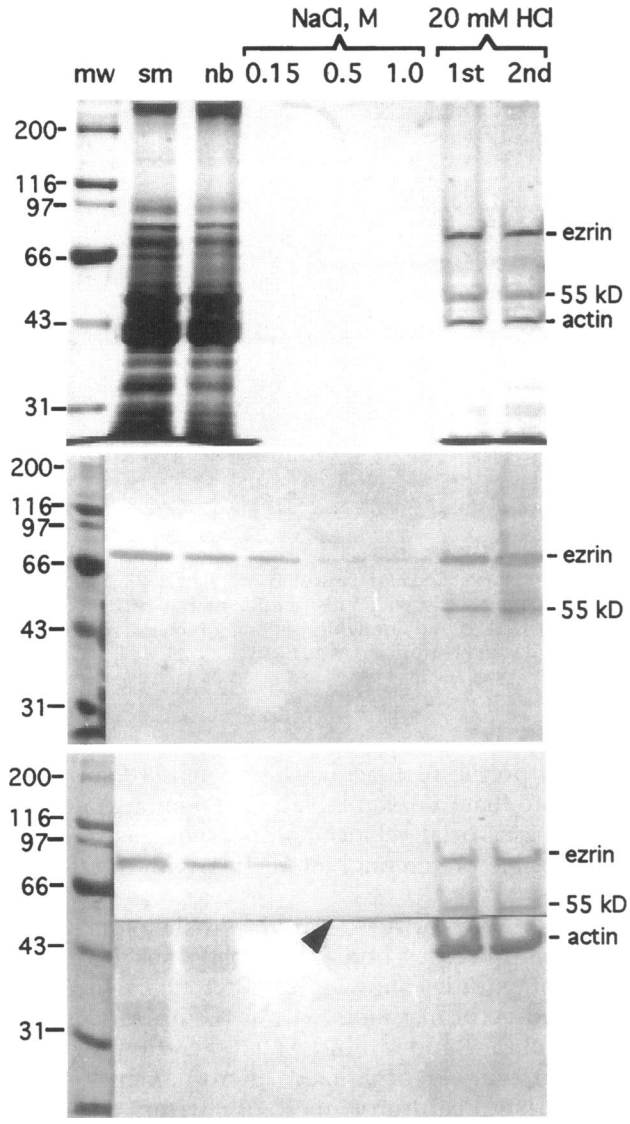

Figure 8. Co-immunoprecipitation of gastric actin with ezrin. The plasma membrane–enriched P1 fraction was extracted with TX-100 and the extract incubated with 6H11-conjugated beads as described in MATERIALS AND METHODS. The beads were washed successively with PBS, 0.5 M NaCl, and 1.0 M NaCl before eluting ezrin with 20 mM HCl in 10% ethylene glycol. All samples were separated by SDS gel electrophoresis. The proteins were either stained with Coomassie blue (upper panel) or transferred onto PVDF membrane for Western blotting (middle and lower panels). Western blots were probed with 6H11 anti-ezrin (middle panel), recognizing 80-kDa ezrin as well as a 55-kDa breakdown product. An identical blot (lower panel) was split at ~50 kDa (arrowhead) and probed with 6H11 (upper half) and anti-actin C4 antibodies (lower half). Lanes: mw, molecular weight standards (labeled on left); sm, starting material TX-100 extract; nb, nonbinding material; 0.15, 0.5, and 1.0, successive NaCl washes; 1st and 2nd, successive 20 mM HCl elutions.

the apical canalicular surface (Forte *et al.*, 1977). These morphological studies suggest that reversible actin-based cytoskeletal modeling underlies the secretory cycle of the parietal cells.

The present immunocytochemical data show that the β-actin isoform is predominantly localized to the apical plasma membrane of the gastric parietal cell, including the tortuous surface of the intracellular canaliculus, and the γ-actin isoform is predominantly localized to the basolateral membrane. Nonparietal gastric epithelial cells also showed a high degree of isoform asymmetry, with the β-actin isoform dominating at the apical surface so that the entire gland lumen was prominently stained by this isoform. A similar pattern of luminal staining was seen when glands were probed with phalloidin to localize F-actin. It should be pointed out that the spatial separation of the β-and γ-actin is not absolute. Some staining of basolateral membranes was always observed with the

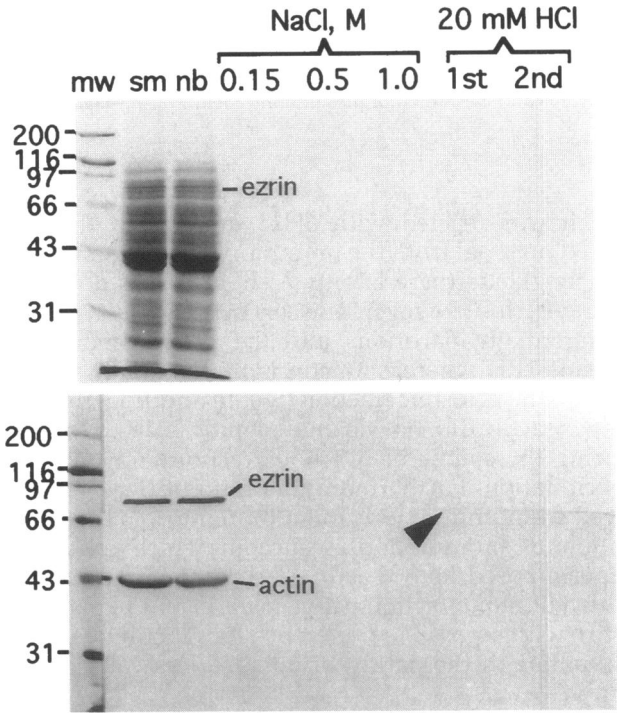

Figure 9. Neither ezrin nor actin are adsorbed to the Affi-Gel 10 beads if an anti-ezrin antibody is not attached. This experiment represents a control for that shown in Figure 8. The P1 membrane fraction was extracted with TX-100 and incubated with Affi-Gel beads that had been coupled with a nonspecific monoclonal antibody that does not recognize parietal cell proteins. The beads were then successively washed with PBS, 0.5 M NaCl, 1.0 M NaCl, and finally 20 mM HCl in 10% ethylene glycol, just as described in Figure 8, and samples were assayed by SDS-PAGE stained with Coomassie blue (upper panel) or transferred onto PVDF membrane for Western blotting (lower panel). The Western blot was probed for ezrin (upper half) or with C4 anti-actin antibody (lower half). Lanes: mw, molecular weight standards (labeled on left); sm, starting material TX-100 extract; nb, nonbinding material; 0.15, 0.5, and 1.0, successive NaCl washes; 1st and 2nd, successive 20 mM HCl elutions.

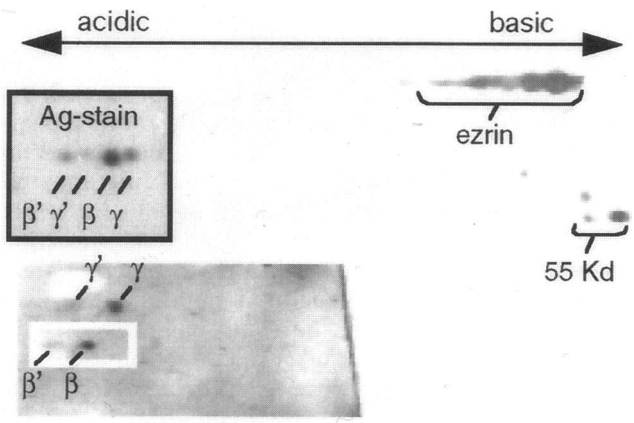

Figure 10. Preferential co-purification of β-actin with ezrin. Ezrin was immuno-purified from the TX-100 extract of the plasma membrane–enriched P1 fraction as described in Figure 7, using 6H11 adsorbed to protein G and then subjected to 2-D electrophoresis. The separated proteins were transferred onto PVDF membrane for Western blotting. The main panel shows a blot probed for ezrin; a small portion was cut from the same blot and probed for the γ-actin isoform (lower left). The 80-kDa ezrin and a series of phosphorylated ezrin isoforms were identified with pI varying from ~6.7 to 6.2. The 55-kDa breakdown product of ezrin was also identified. The portion of the blot probed for γ-actin shows a main spot (γ) and a minor spot (γ'). Separate blots probed for the β-actin isoform (white-bordered inset) also identified major (β) and minor spots (β'). When 2-D gels were silver stained, four spots could be identified (black-bordered inset) corresponding to the major and minor spots of both the β- and γ-actin isoforms (labeled β, β', γ, and γ'). Similar silver-stained gels from four preparations were used for quantitation by densitometry.

β-actin antibody, and we occasionally observed a low level of γ-actin staining within the canalicular membrane although the basolateral staining was overwhelming. Because we never observed cross-reactivity between the isoform-specific antibodies in our Western blot analyses, the immunocytolocalization data appear to represent the true distribution of actin isoforms in gastric epithelial cells. Thus, we conclude that spatial distribution of cytoplasmic β- and γ-actin isoforms in parietal cells is polarized in the two distinct membrane regions, and may implicate some role for functional divergence of actin isoforms in the phenomenon of epithelial cell polarity. Asymmetry of actin isoform distribution in gastric glands and parietal cells is supported by the densitometric assays of isoforms in cell fractions. G-actin, purified from the supernatant fraction derived from gastric mucosal homogenates, was assayed to contain a slight excess of γ-actin over the β-actin isoform (β-actin/γ-actin = 0.73 ± 0.09). On the other hand, the low speed membrane fraction (P1), mainly containing filamentous actin, was predominantly of the β-actin isoform (β-actin/γ-actin = 2.26 ± 0.32).

The three-dimensional structure of cytoplasmic β-actin, in complex with profilin, was recently solved (Schutt *et al.*, 1993). Although its primary sequence is generally similar to skeletal α-actin, cytoplasmic β-actin displays several structural differences. These include the following: the N-terminal conformation of β-actin bearing a turn rather than the helical structure for skeletal α-actin; distinct rotational differences within subdomains of the isoforms; and differences in side-chain orientation at residues 38 to 52. Physiological interpretation of these structural distinctions is still under debate (Rozycki *et al.*, 1994), but functional differences in the interaction of actin isoforms with actin binding proteins have been reported. Larsson and Lindberg (1988) showed that nonmuscle actin isoforms, cytoplasmic β-actin and γ-actin, have higher affinity to bind profilin (K_d ~10^{-8} M) than sarcomeric actin (K_d ~4×10^{-6} M), and that profilin interaction with the nonmuscle isoforms was regulated by Mg^{2+}. Rozycki *et al.* (1991) further demonstrated that profilin preferentially binds to cytoplasmic β-actin compared with γ-actin. The ratio of β- to γ-actin isoforms is elevated in ezrin-rich fractions from gastric glands compared with that of whole cell lysates, suggesting that ezrin might preferentially bind to β-actin–based filaments. This might be another case where actin isoforms selectively interact with their accessory proteins. Indeed, distinctive intracellular distribution of the isoforms demands that highly selective interactions occur. Bretscher observed (1983) that ezrin cosedimented with filamentous skeletal muscle actin in vitro only at low ionic strength. However, in view of the highly selective differences in affinity between var-

Table 1. Ratios of β-actin to γ-actin isoforms in various fractions, and extracts of fractions, from gastric glands.

Cell fraction	β/γ ratio	n
Whole cell lysate	1.35±0.07	3
Cytosol	0.73±0.09	5
Membranes (P1)	2.26±0.32	4
Total membrane extract	2.24±0.61	4
Immunoprecipitate with ezrin	2.14±0.32	4

Preparation of the cytosol and membrane (P1) fractions are described in MATERIALS AND METHODS. The total membrane extract was the starting material for the immunoprecipitation experiments with anti-ezrin mAb 6H11, and was derived from the P1 membranes by TX-100 extraction, as described. The immunoprecipitate was eluted from the anti-ezrin column with acid. All fractions were subjected to 2-D electrophoresis as shown in Figures 1 and 10. Spots were identified as β-actin or γ-actin and assayed by densitometry to determine the relative β/γ actin ratio in each case. In the case of relatively pure fractions, like cytosol and immunoprecipitate, densitometry was carried out on silver stained 2-D gels; for the other, cruder fractions densitometry was carried out on Western blots probed with an antibody that recognizes all actin isoforms. n = the number of separate preparations assayed.

ious actin isoforms and another actin binding protein, profilin (Larsson and Lindberg, 1988), it is not surprising that the ezrin-β-actin complex could be sustained, even at high ionic strength.

Compelling evidence for the role that nonmuscle actin plays in regulating cell motility and cytoskeletal architecture derives from several lines of evidence, including the use of isoform-specific antibodies, cDNA transfection, mRNA localization, and mutant analyses (Herman 1993). Examination of the wound healing process in endothelial cells showed that the β-actin isoform, together with its mRNA, was exclusively distributed in leading lamellae, membrane ruffles, and advancing pseudopods (Hoock *et al.*, 1991). Functional diversity of β-actin and γ-actin isoforms was demonstrated in C2 myoblasts where overexpression of the human β-actin isoform gene induced an increase in cell surface area and loss of stress fibers, whereas overexpression of the γ-actin isoform was associated with a decreased surface area (Schevzov *et al.*, 1992). To verify the role of β-actin in generating an enlarged cell phenotype, these authors further demonstrated that transfection of C2 myoblasts with mutant β-actin caused the disruption of the actin microfilament network and a decrease in membrane surface area similar to that of C2 cells that were transfected with wild-type γ-actin. Thus, these data suggest that distinct functional divergence of β-actin and γ-actin might be involved in the formation of specific actin-based cytoarchitecture (i.e., stress fibers, cortical microfilaments). Moreover, a putative role for cytoplasmic β-actin in cell motility was suggested by experiments in which cytochalasin-sensitive KB cells were transfected with exogenous β-actin, which contained two mutated amino acids ($^{Val}139^{Met}$ and $^{Ala}295^{Asp}$). Expression of this mutated β-actin cDNA in KB cells minimized the expression of wild-type β-actin, without any influence on γ-actin, and gave rise to a resistance to cytochalasin D treatment (Ohmori *et al.*, 1992). Stimulation of acid secretion by parietal cells is associated with large increases in the length of apical microvilli and in the surface area of the apical plasma membrane, whereas no obvious morphological change occurs at the basolateral plasma membrane (Forte and Soll, 1989). The differentiated localization of actin isoforms in parietal cells might provide a basis for two distinct functional domains. Given the polarized distribution of β-actin to the apical surface and γ-actin to the basolateral membrane established here, together with distinct functional diversities of β- and γ-actin isoforms, we propose that the networks of β- and γ-actin–based microfilaments function distinctly in gastric parietal cells upon the stimulation of acid secretion.

Data for amino acid sequence reveals that ezrin is a member of the band 4.1 superfamily, which includes erythrocyte protein band 4.1, talin, protein tyrosine phosphatase, the neurofibromatosis tumor-suppressor, and the ezrin-radixin-moesin (ERM) family. Band 4.1 is a membrane-cytoskeletal linker that connects the integral membrane protein glycophorin to the subcortical actin-spectrin complex. Talin links the fibronectin receptor to the actin cytoskeleton via vinculin and α-actinin (Rees *et al.*, 1990). Radixin, one ERM family member originally isolated from the adherens junction of hepatocyte, has shown actin-binding activity via capping the barbed end of actin filament in vitro (Tsukita *et al.*, 1989). Those authors subsequently showed that radixin is highly concentrated at the cleavage furrow in a variety of culture cells during cytokinesis, which implies that radixin might modulate the actin filament-plasma membrane interaction at the furrow (Sato *et al.*, 1991). The subcellular localization of ezrin and its sequence homology to protein 4.1 and talin suggested that ezrin also connects plasma membrane and actin-based cytoskeleton (Gould *et al.*, 1989). Although a great deal of effort has been spent to verify such an hypothesis, only recently have Louvard and his colleagues shown that the N-terminal half of ezrin determines the plasma membrane association whereas the C-terminal half is responsible for actin-cytoskeletal association, as judged by immunocytochemistry and detergent extraction as well as cytochalasin D treatment (Algrain *et al.*, 1993). Their data indicate that ezrin is a cytoskeleton-membrane linker present in the cortical cytoskeleton, and ezrin has at least one site to interact with an actin filament. During preparation of this manuscript, Turunen *et al.* (1994) reported their studies on partial length ezrin-GST fusion proteins, demonstrating that the C-terminal end of ezrin was critical for binding to F-actin. The present results provide the first evidence demonstrating a biochemical interaction between cytoplasmic actin and full-length ezrin isolated in situ, although the data could not address the nature of ezrin-actin interaction, direct vs. indirect. In fact, as seen in Table 1, the composition of actin isoforms in complex with ezrin was not altered significantly from the crude membrane source during the detergent extraction and immunopurification. The extent to which the physiological regulation of ezrin-actin interactions may depend upon factors, such as phosphorylation, actin isoform specificity, and ezrin homodimerization, remains a subject for future study.

It was noted that a substantial amount of the gastric β- and γ-actin isoforms occurred with multiple pI's, suggesting the possibility of some phosphorylation of gastric actin. Alternatively, those variants might represent actin isoforms that underwent post-translational modification as reported by Leavitt *et al.* (1980). Howard *et al.* (1993) showed that an increase in tyrosine phosphorylation of actin occurred in parallel to developmentally induced shape changes in *Dictyostelium* cells. However, actin phosphorylation has not

been reported in vertebrates, thus it will be of interest to specifically test whether gastric actin is phosphorylated, and whether it has functional significance in mediating ezrin-actin association during the course of acid secretion in parietal cells. For ezrin, Krieg and Hunter (1992) have carefully mapped the tyrosine phosphorylation sites that were correlated to the onset of EGF stimulation in A431 cells. Thus, the membrane ruffling of EGF-stimulated A431 cells occurs in parallel to tyrosine phosphorylation in ezrin, presumably at Tyr^{145} and Tyr^{353}. Interestingly, serine phosphorylation in ezrin has been correlated to the onset of apical membrane-cytoskeleton reorganization in gastric parietal cells upon stimulation, however, it is unclear whether the phosphorylation of ezrin modulates the interaction between membrane and cortical actin cytoskeleton.

Cell biologists have long been fascinated by how cells sort proteins into specific cellular compartments and how that specific distribution is retained. A great deal is known about the secretory machinery by which integral membrane proteins are sorted. In contrast, much less is known about the partitioning of cytosolic proteins (Wilhelm and Vale, 1993). It is becoming clear that the transport of mRNAs rather than translated proteins plays a major role in the distribution of cytosolic proteins. The sorting of mRNA for the actin isoforms provides an interesting system to study the mRNA localization machinery (Singer, 1992). Actin mRNA distribution depends on a pre-existing actin-based filament because the disruption of this network by cytochalasin, but not colcemid, alters its subcellular localization (Sundell and Singer, 1990). More recently, Singer's group revealed two nucleotide segments, within β-actin mRNA, that are responsible for the β-actin mRNA localization and for the cell phenotype determination (Kislauskis *et al.*, 1994). A polarized distribution of cytoplasmic β-actin mRNA has been reported in intestinal epithelial cells (Cheng and Bjerknes, 1989). Yeh and Svoboda (1994) showed that β-actin mRNA is colocalized with filamentous actin in apical microvilli of embryonic corneal epithelia. Because of the use of nonspecific probes for actin staining, it is difficult to judge whether the total actin signals are composed of a single actin isoform or two different isoforms (Yeh and Svoboda, 1994). More recently, Gunning's group showed that myoblasts sort the β- and γ-actin mRNAs, but not the translated proteins, into different intracellular compartments, and that the peripheral location of β-actin mRNA is regulated by serum with no apparent effect on γ-actin localization (Hill *et al.*, 1994). The authors further showed that serum-induced β-actin mRNA distribution is mediated through the GTPase signalling pathway. A similar conclusion was drawn by Singer's group in observing that PDGF-induced β-actin mRNA was dependent on tyrosine kinase activity for redistribution in chicken embryo fibroblast and that the relocation of steady-state β-actin mRNA in serum-containing media was inhibited by modulators of protein kinase A and C (Latham *et al.*, 1994). These lines of evidence suggest that the signal transduction events modulate the dynamics of β-actin mRNA localization. It would be tempting to test the localization of mRNAs for β- and γ-actin in relation to the corresponding protein and the regulation during the stimulation-mediated volatile membrane reorganization in gastric parietal cells where two actin isoforms are polarized. If the mRNA co-distributes with its protein by using the same isoform filaments, the docking machinery must somehow select the favorite filament either by isoform-specific binding proteins including isoform-specific motor proteins, or by distinct properties of filaments derived from different isoforms.

Taken together, our present work reveals for the first time that cytoplasmic β- and γ-actin isoforms co-exist differentially in gastric epithelial cells, with a polarized distribution pattern. Cytoplasmic β-actin predominates in the secretory canaliculus of parietal cells and the apical plasma membranes of all glandular cells lining the gastric lumen. The cytoplasmic γ-actin isoform is sequestered near the basolateral membrane sites of parietal cells with diminished localization to secretory canaliculi and very little representation along the luminal surface. Moreover, the subcellular distribution profile of the β-actin isoform closely superimposes onto that of ezrin within the parietal cells. Finally, the immunoprecipitation of native ezrin demonstrates an ezrin-gastric actin association, with the suggestion that the association might be preferential for the β-actin isoform. Given that stimulation-regulated volatile membrane remodeling occurs exclusively in apical plasma membrane and the distinct spatial distribution of the actin isoforms, we propose that β-and γ-actin–based filamentous networks are functionally distinct in gastric parietal cells, especially in response to the stimulation of acid secretion.

ACKNOWLEDGMENTS

We thank Dr. James Lessard for the C4 antibody and Dr. Hans-Peter Hauri for the G1/136 antibody. This work was supported in part by grants from the National Institute of Diabetes and Digestive and Kidney Diseases, DK-38972 and DK-10141, and by grants from the Swiss National Science Foundation, 31–34062.92 and 31–40372.94. A portion of this work was presented in abstract form to the American Society for Cell Biology, December 1993 and 1994.

REFERENCES

Algrain, M., Turunen, O., Vaheri, A., Louvard, D., and Arpin, M. (1993). Ezrin contains cytoskeleton and membrane binding domains accounting for its proposed role as a membrane-cytoskeletal linker. J. Cell Biol. *120*, 129–139.

Berglindh, T., and Obrink, K.J. (1976). A method for preparing isolated glands from the rabbit gastric mucosa. Acta Physiol. Scand. *96*, 150–159.

Black, J.A., Forte, T.M., and Forte, J.G. (1982). The effects of microfilament disrupting agents on HCl secretion and ultrastructure of piglet gastric oxyntic cells. Gastroenterology *83*, 595–604.

Bretscher, A. (1983). Purification of an 80,000-dalton protein that is a component of the isolated microvillus cytoskeleton, and its localization in nonmuscle cells. J. Cell Biol. *97*, 425–32.

Carrington, W.A., Fogarty, K.E., and Fay, F.S. (1990). 3-D fluorescence imaging of single cells using image restoration. In: Noninvasive Techniques in Cell Biology, ed. K. Foskett and S. Grinstein, New York, NY: Wiley-Liss, 53–72.

Chaponnier, C., and Gabbiani, G. (1989). Gelsolin modulation in epithelial and stromal cells of mammary carcinoma. Am. J. Pathol. *134*, 597–603.

Cheng, H., and Bjerknes, M. (1989). Asymmetric distribution of actin mRNA and cytoskeletal pattern generation in polarized epithelial cells. J. Mol. Biol. *210*, 541–549.

DeNofrio, D., Hoock, T.C., and Herman, I.M. (1989). Functional sorting of actin isoforms in microvascular pericytes. J. Cell Biol. *109*, 191–202.

Eilers, U., Klumpermen, J., and Hauri, H-P. (1989). Nocodazole, a microtubule-active drug, interferes with apical protein delivery in cultured intestinal epithelial cells (Caco-2). J. Cell Biol. *108*, 13–22.

Fay, F.S., Carrington, W., and Fogarty, K.E. (1989). Three-dimensional molecular distribution in single cells analyzed using using the digital imaging microscope. J. Microsc. *153*, 133–149.

Firtel, R.A. (1981). Multigene families encoding actin and tubulin. Cell *24*, 6–7.

Forte, J.G., and Soll, A. (1989). Cell biology of hydrochloric acid secretion. In: Handbook of Physiology–The Gastrointestinal System, vol III, chapter 11, ed. J.G. Forte, Bethesda, MD: American Physiological Society, 207–228.

Forte, T.M., Machen, T.E., and Forte, J.G. (1977). Ultrastructural changes in oxyntic cells associated with secretory function: a membrane-recycling hypothesis. Gastroenterology *73*, 941–55.

Gould, K.L., Bretscher, A., Esch, F.S., and Hunter, T. (1989). cDNA cloning and sequencing of the protein-tyrosine kinase substrate, ezrin, reveals homology to band 4.1. EMBO J. *8*, 4133–4142.

Hanzel, D., Reggio, H., Bretscher, A., Forte, J.G., and Mangeat, P. (1991). The secretion-stimulated 80K phosphoprotein of parietal cells is ezrin, and has properties of a membrane cytoskeletal linker in the induced apical microvilli. EMBO J. *10*, 2363–2373.

Hanzel, D.K., Urushidani, T., Usinger, W.R., Smolka, A., and Forte, J.G. (1989). Immunological localization of an 80-kDa phosphoprotein to the apical membrane of gastric parietal cells. Am. J. Physiol. *256*(Gastrointest. Liver Physiol. *19*), G1082–G1089.

Herman, I. (1993). Actin isoforms. Curr. Opin. Cell Biol. *5*, 48–55.

Herman, I.M. (1988). Developing probes and methods for morphological and biochemical analyses of cytoskeletal elements in vascular cells. CRC Crit. Rev Anat. Sci. *1*, 133–148.

Herman, I.M., and D'Amore, P.A. (1985). Microvascular pericytes contain muscle and nonmuscle actins. J. Cell Biol. *101*, 43–52.

Hill, M.A., and Gunning, P. (1993). Beta and gamma actin mRNAs are differentially located within myoblasts. J. Cell Biol. *122*, 825–832.

Hill, M.A., Schedlich, L., and Gunning, P. (1994). Serum-induced signal transduction determines the peripheral location of β-actin mRNA within the cell. J. Cell Biol. *126*, 1221–1230.

Hoock, T.C., Newcomb, P.M., and Herman, I.M. (1991). β actin and its mRNA are localized at the plasma membrane and the regions of moving cytoplasm during the cellular response to injury. J. Cell Biol. *112*, 653–664.

Howard, P.K., Sefton, B.M., and Firtel, R.A. (1993). Tyrosine phosphorylation of actin in *Dictyostelium* associated with cell-shape changes. Science *259*, 241–244.

Kislauskis, E.H., Zhou, X., and Singer, R.H. (1994). Sequences responsible for intracellular localization of β-actin messenger RNA also affect cell phenotype. J. Cell Biol. *127*, 441–451.

Krieg, J., and Hunter, T. (1992). Identification of the 2 major epidermal growth factor-induced tyrosine phosphorylation sites in the microvillar core protein ezrin. J. Biol. Chem. *267*, 19258–19265.

Latham, V.M., Jr., Kislauskis, E.H., Singer, R.H., and Ross, A.F. (1994). β-actin mRNA localization is regulated by signal transduction mechanism. J. Cell Biol. *126*, 1211–1219.

Larsson, H., and Lindberg, U. (1988). The effect of divalent cations on the interaction between calf spleen profilin and different actins. Biochem. Biophys. Acta. *953*, 95–105.

Lessard, J.L., Scheffter, S., Engel, L., and Tepperman, K. (1983). Immunofluorescent localization of actins in differentiating chick myoblasts. J. Cell Biol. *97*, 74a (abstract).

Leavitt, J., Leavitt, A., and Attallah, A.M. (1980). Dissimilar modes of expression of β- and γ-actin in normal and leukemic human T lymphocytes. J. Biol. Chem. *255*, 4984–4987.

North, A.J., Gimona, M., Lando, Z., and Small, J.V. (1994). Actin isoform compartments in chicken gizzard smooth muscle cells. J. Cell Sci. *107*, 445–455.

O'Farrell, P.H. (1975). High resolution two-dimensional electrophoresis of proteins. J. Biol. Chem. *250*, 4007–4021.

Ohmori, H., Toyama, S., and Toyama, S. (1992). Direct proof that the primary site of action of cytochalasin on cell motility is actin. J. Cell Biol. *116*, 933–941.

Otey, C.A., Kalnoski, M.H., Lessard, J.L., and Bulinski, J.C. (1986). Immunolocalization of gamma isoform of nonmuscle actin in culture cells. J. Cell Biol. *102*, 1726–1737.

Pardo, J.V., Pittenger, M.F., and Craig, S.W. (1983). Subcellular sorting of isoactins: selective association of γ actin with skeletal muscle mitochondria. Cell *32*, 1093–1103.

Reenstra, W.W., and Forte, J.G. (1990). Isolation of H, K-ATPase-containing membranes from the gastric oxyntic cell. Methods Enzymol. Biomembr. *192*, 151–164.

Rees, D.J., Ades, S.E., Singer, S.J., and Hynes, R.O. (1990). Sequence and domain structure of talin. Nature *347*, 685–689.

Rozycki, M., Myslik, J.C., Schutt, C.E., and Lindberg, U. (1994). Structural aspects of actin-binding proteins. Curr. Opin. Cell Biol. *6*, 87–95.

Rozycki, M., Schutt, C.E., and Lindberg, U. (1991). Affinity chromatography-based purification of profilin:actin. Methods Enzymol. *196*, 100–118.

Sato, N., Yonemura, S., Obinata, T., Tsukita, Sa., and Tsukita, Sh. (1991). Radixin, a barbed end-capping actin-modulating protein, is concentrated at the cleavage furrow during cytokinesis. J. Cell Biol. *113*, 321–330.

Schevzov, G., Lloyd, C., and Gunning, P. (1992). High level expression of transfected β-actin and γ-actin genes: differentially impacts on myoblast cytoarchitecture. J. Cell Biol. *117*, 775–785.

Schutt, C., Myslik, L., Rozycki, M., Goonesekere, N., and Lindberg, U. (1993). The structure of crystalline profilin:β-actin. Nature *365*, 810–816.

Singer, R.H. (1992). The cytoskeleton and mRNA localization. Curr. Opin. Cell Biol. *4*, 15–19.

Sundell, C.L., and Singer, R.H. (1990). Actin messenger RNA localizes in the absence of protein synthesis. J. Cell Biol. *111*, 2397–2403.

Toyama, S., and Toyama, S. (1984). A variant form of beta-actin in a mutant of KB cells resistant to cytochalasin B. Cell *37*, 609–614.

Tsukita, Sa., Hieda, Y., and Tsukita, Sh. (1989). A new 82-kD barbed end-capping protein (radixin) localized in the cell-to-cell adherens junction: purification and characterization. J. Cell Biol. *108*, 2369–2382.

Turunen, O., Wahlström, T., and Vaheri, A. (1994). Ezrin has a COOH-terminal actin-binding site that is conserved in the ezrin protein family. J. Cell Biol. *126*, 1445–1453.

Urushidani, T., Hanzel, D.K., and Forte, J.G. (1989). Characterization of an 80-kDa phosphoprotein involved in parietal cell stimulation. Am. J. Physiol. *256*, 1070–1081.

Vandekerckhove, J. (1990). Actin-binding proteins. Curr. Opin. Cell Biol. *2*, 41–50.

Vandekerckhove, J., and Weber, K. (1978). At least six different actins are expressed in a higher mammal: an analysis based on the amino acid sequence of the amino-terminal tryptic peptide. J. Mol. Biol. *126*, 783–802.

Vandekerckhove, J., and Weber, K. (1981). Actin typing on total cellular extracts: a highly sensitive protein-chemical procedure able to distinguish different actins. Eur. J. Biochem. *113*, 595–603.

Wilhelm, J.E., and Vale, R.D. (1993). RNA on the move: the messenger RNA localization pathway. J. Cell Biol. *123*, 269–274.

Wolosin, J.M., Okamoto, C., Forte, T.M., and Forte, J.G. (1983). Actin and associated proteins in gastric epithelial cells. Biochim. Biophys. Acta *761*, 171–182.

Yao, X., Thibodeau, A., and Forte, J.G. (1993). Ezrin-calpain interaction in gastric parietal cells. Am. J. Physiol. *265*, C36–46.

Yeh, B., and Svoboda, K.K.H. (1994). Intracellular distribution of β-actin mRNA is polarized in embryonic corneal epithelia. J. Cell Sci. *107*, 105–115.